

Dear Dr. Shemesh,

Please find our reply to the reviewer's comments below. We are grateful for the thorough comments and are convinced that we have addressed all points satisfactorily.

Best wishes

Gerald Langer (on behalf of all authors)

Detailed reply to the reviewer's comments:

Reply to Y. Dauphin:

REPLY: We would like to thank Y. Dauphin for this thorough comment and are confident that we have satisfactorily addressed all the points below.

Nevertheless, some questions persist.

First, only some specialists are able to identify the species of *Patella*. Only small details are important, and because even the shells of living animals are eroded or encrusted, color patterns are not well visible. Several species often co-exist in a single site. Thus, the taxonomy of "*Patella*" is still controversial. The morphology (inner and outer views) of the samples will be useful.

REPLY: *Patella* samples were checked by Francesco Paolo Patti (SZN, Ischia) who confirmed the taxonomy. We included photographs of the shells we analysed in the revised manuscript (Figure S1).

2nd:

microstructural observations are missing. The structure of the shell of this genus is unique: the crossed lamellar layer (the most common structure in Mollusks) is calcitic.

Some sublayers are aragonitic. But the main part of aragonite is a prismatic layer related to the muscle insertion (myostracum). The absence of thin sections or SEM pictures does not allow the reader to understand what is the structure of what is called "aragonite" in the manuscript.

REPLY: While we agree that it would be, per se, interesting to have information on the microstructure of the shells, this information is irrelevant with respect to the scope of the present manuscript. For our purpose it is sufficient to know which parts of the shells are aragonitic and which are calcitic. We are looking forward to addressing the question of microstructure in the future, though.

Third: despite the high quality of Raman analyses, other cheaper and faster techniques are available: BSE SEM images with or without staining (Feulgen, spatial resolution about 1 micron), staining of thin sections.

REPLY: Since several techniques were available, we had to make a choice. We did choose Raman microscopy.

Fourth: we have no data about the age of the samples, and the duration of their exposure to the acidic site.

REPLY: The samples were exposed to the respective sites (normal versus low pH) all their lives. The exact age of the samples is unknown to us. They are probably several years old.

Fifth: there is no data about the parameters of the sea water (salinity, temperature, agitation...); these parameters play a role in the life of the animal, as the nutrient does.

Some decades ago, it was shown that the calcitic/aragonitic ratio in *Mytilus* shell de-

depends on the sea water salinity (Dodd in the 60's). This controversial interpretation was not confirmed and it has been shown that other factors play a role. It seems there is a similar situation here. The authors of the manuscript deal with a topic regularly mentioned in all the past and present, national and international projects in which the future climate is concerned. They do not compare their results to what is described for other molluscs. At last, the observations are not sufficient enough to be so affirmative regarding the conclusions. The authors must discuss other hypotheses.

REPLY: We agree insofar that data based on field samples do not warrant the same degree of interpretative certainty as data based on experimental samples. Having said that, the field samples we used are very special and probably as close as one can get to a laboratory experiment. The reason for this is that the Ischia CO₂ vent site features a classical DIC-manipulation scenario (for details see e.g. Hoppe et al. 2011) without disturbing secondary influences. We have added a paragraph dealing with possible secondary influences:

“We ascribed the changes in shell mineralogy and shell thickness of our samples to seawater carbonate chemistry changes. Since these are field samples, as opposed to experimental samples, possible secondary influences have to be considered. For *Mytilus* it was shown that maybe salinity, but certainly temperature influences the aragonite/calcite ratio (Dodd 1966, Eisma 1966). The latter is also true for *Patella* (Cohen and Branch 1992). In our case, however, both temperature and salinity at the two sites (Figure 1) were the same at any given time (Table 1, Cigliano et al. 2010, Hall-Spencer et al. 2008, Rodolfo-Metalpa et al. 2011), and we conclude that these two parameters did not influence the aragonite/calcite ratio of our samples. Also both the control site and the low pH site we sampled at Ischia are sheltered so that there is no difference in wave action, which could potentially influence shell architecture. Furthermore, it was suggested that the concentrations of inorganic ions such as Mg and Sr can influence the mineralogy of marine calcifying organisms (Watabe 1974). Since salinity was constant in our case, the concentrations of major ions such as Mg and Sr were likewise, and their influence can be ruled out. On the other hand, shells from the low pH site clearly are corroded (see above), so there is a massive impact of seawater carbonate chemistry on the organism. Taken together with the constancy of other environmental parameters, that leads us to conclude that carbonate chemistry changes are the best explanation for the changes in shell mineralogy and shell thickness of our samples.”

The effect of the corrosive water at the low pH site is further illustrated by a number of images at our disposal. We attach a few examples to this reply, but don't think it is necessary to include them in the manuscript, because the corrosive nature of the low pH site is already well documented (see page 12573, line 23 of our manuscript).

Figure Caption:

Fig. 1 Gastropod molluscs living adjacent to shallow water CO₂ seeps off Ischia showing severely eroded shells due to the corrosive effects of the seawater a) *Hexaplex trunculus*, b) *Osilinus turbinata* and c) *Patella*

caerulea. At control sites these gastropod species were common but were never found with dissolved shells like these

References

Cigliano, M; Gambi, Maria Cristina; Rodolfo-Metalpa, Riccardo; Patti, F P; Hall-Spencer, Jason M (2010): Effects of ocean acidification on invertebrate settlement at volcanic CO₂ vents. *Marine Biology*, 157(11), 2489-2502

Cohen, A.L., Branch, G.M. (1992) Environmentally controlled variation in the structure and mineralogy of *Patella granularis* shells from the coast of southern Africa: implications for palaeotemperature assessments, *Palaeogeography, Palaeoclimatology, Palaeoecology*, Volume 91, Pages 49-57

Dodd, J.R. (1966) The Influence of Salinity on Mollusk Shell Mineralogy: A Discussion. *The Journal of Geology*, Vol. 74, pp. 85-89

Eisma, D. (1966) The Influence of Salinity on Mollusk Shell Mineralogy: A Discussion. *The Journal of Geology*, Vol. 74, pp. 89-94

Hall-Spencer, J. M., Rodolfo-Metalpa, R., Martin, S., Ransome, E., Fine, M., Turner, S. M., Rowley, S. J., Tedesco, D., and Buia, M.-C. (2008) Volcanic carbon dioxide vents show ecosystem effects of ocean acidification, *Nature*, 454, 96–99

Hoppe, C., Langer, G. and Rost, B. (2011) *Emiliana huxleyi* shows identical responses to elevated pCO₂ in TA and DIC manipulations, *Journal of Experimental Marine Biology and Ecology*, 406 (1), 54-62

Rodolfo-Metalpa, R., Houlbreque, F., Tambutte, E., Boisson, F., Baggini, C., Patti, F. P., Jeffree, R., Fine, M., Foggo, A., Gattuso, J.-P., and Hall-Spencer, J. M. (2011) Coral and mollusc resistance to ocean acidification adversely affected by warming, *Nature Climate Change*, 1, 308–312

Watabe, N. (1974) Crystal growth of calcium carbonate in biological systems, *Journal of Crystal Growth*, Volumes 24–25, Pages 116-122

End of Reply to C4853Interactive comment on Biogeosciences Discuss., 11, 12571, 2014.

Reply to referee 2:

Reply: We would like to thank Referee 2 for this constructive comment. We have addressed all the points below.

Remarks:

- p2 l.10-12: the formulation is quite intriguing : the calcite layers still keep growing in thickness. (or not ?) cf. comments below.

Reply: We cannot be sure. It appears to us that the calcite layers might indeed keep growing in thickness, but only during elongation growth (i.e. “normal growth”) as opposed to what we have called “enhanced” or “compensatory” shell production. Since we cannot know whether the material produced during compensatory shell production represents growth layers or structural layers, we substituted “parts” for “layers” in the abstract. That makes clear that there is a vagueness here.

- p8 l.11: " inside " (center of the shell) or " inner side " (the whole growth surface of the shell) ?

Reply: The “inner” side. We changed the word. It is not the whole growth surface, however, but only the aragonitic parts, as we described in the following sentences.

- p8 l.21-23: " This mechanism allows for compensatory shell thickening through the deposition of additional layers on the inside of the shell ".

Not clear to me. What does " layer " mean here ? Growth layers or structural layers ? Patella shells can display up to 7 structural layers, displaying crossed lamellar (XL) (aragonite), cross-foliated (CF) (calcite) or myostracal (M) microstructures (McClintock, 1967). They are all deposited synchronously, at each growth increment (" growth layer"), on the inner surface of the shell. Does the authors mean thicker (and not " additional ") growth layers in the center of the shell than in the border (therefore, just different calcification rates in the two zones) ? Or is there a specific deposit (additional " structural " layers) that recovers the center of the shell, in a mechanism that could be more related to shell -remobilization or –repair processes ? These latter are indeed quite frequently observed in gastropod shells (and display specific microstructures, ex. Fleury et al, 2008). It is hard to decipher without a microstructural investigation, that would be much welcomed to validate the mechanism proposed by the authors. The absence of such an investigation is intriguing, as some features are already visible in the Confocal Raman Microscopy pictures provided (in Fig 4 : growth lines, cross-foliated

lamellae in M+2/M+3 layers, etc.). Why not provide some more resolute maps ? It seems like then present manuscript acts like a preliminary study, meaning to precede a more complete microstructural investigation. It have no objection to it, given it is clearly stated in the manuscript (in the conclusion perhaps).

Reply: As referee 2 correctly says, we cannot know this without a microstructural investigation, which is indeed a follow up study. We did as suggested by referee 2 and stated that in the conclusion. We also added the following to clarify:

“We do not know whether the additional layers are structural layers. One possibility is that the layers we call “additional” are similar to the layers related to shell repair in *Haliotis* (Fleury et al. 2008).”

- p9: actually, the conclusion is just a copy/paste of p6|20-25, making it redundant and not very useful.

Reply: We modified the Conclusion. It now reads:

“Polymorph distribution analyses of complete cross sections of *Patella caerulea* shells from a CO₂ vent site at Ischia revealed that this species counteracts shell dissolution in corrosive waters by enhanced production of aragonitic shell layers. The question whether these layers represent structural layers will be the subject matter of an upcoming microstructural investigation.”

- I am not native english, but the spelling and syntax seem fine to me.

Interactive comment on Biogeosciences Discuss., 11, 12571, 2014.

C5552

Limpets counteract ocean acidification induced shell corrosion by thickening of aragonitic shell layers

Gerald Langer¹, Gernot Nehrke², Cecilia Baggini³, Riccardo Rodolfo-Metalpa⁴, Jason Hall-Spencer³,

5 Jelle Bijma²

¹Department of Earth Sciences, Cambridge University, Cambridge, UK

²Biogeosciences, Alfred Wegener Institute, Bremerhaven, Germany

³School of Marine Science and Engineering, University of Plymouth, Plymouth, UK

10 ⁴CoRéUs, Institut de Recherche pour le Développement, Centre IRD de Noumea, Noumea, New Caledonia

ABSTRACT

Specimens of the patellogastropod limpet *Patella caerulea* were collected within (pH_{low}-shells) and outside (pH_n-shells) a CO₂ vent site at Ischia, Italy. Four pH_{low}-shells and
15 four pH_n-shells were sectioned transversally and scanned for polymorph distribution by means of confocal Raman microscopy. The pH_{low}-shells displayed a twofold increase in aragonite area fraction and size normalised aragonite area. Size normalised calcite area was halved in pH_{low}-shells. Taken together with the increased apical and the decreased flank size normalised thickness of the pH_{low}-shells, these data led us to conclude that low pH exposed *P.*
20 *caerulea* specimens counteract shell dissolution by enhanced shell production. The latter is different from normal elongation growth and proceeds through addition of aragonitic parts ~~layers~~ only, while the production of calcitic parts ~~layers~~ is confined to elongation growth. Therefore aragonite cannot be regarded as a per se disadvantageous polymorph under ocean acidification conditions.

25

1. INTRODUCTION

There is general consensus that anthropogenic CO₂ emissions lead to decreasing surface ocean pH and carbonate ion concentration, a process termed ocean acidification (e.g. Royal Society, 2005). The latter entails a decrease in seawater saturation state with respect to calcium carbonate. Calcium carbonates occur in the form of different polymorphs, the most resistant to dissolution being calcite, followed by aragonite. It was proposed that by the year 2100 the subarctic Pacific Ocean and the entire Southern Ocean will be under-saturated with respect to aragonite (Orr et al., 2005). Wintertime aragonite under-saturation in the Southern Ocean may even occur as early as 2030 (McNeil and Matear, 2008). Since many marine organisms use aragonite or calcite to build their shells, there have been concerns regarding the vulnerability of these organisms to ocean acidification. The fact that aragonite is more soluble than calcite has led to the widely held notion that aragonite producers are more vulnerable to ocean acidification than calcite producers (Field et al., 2011; Gattuso and Hansson, 2011; Royal Society, 2005). The extreme sensitivity of aragonitic pteropods to dissolution (Bednarsek et al., 2012) seems to support this view. Some molluscs, e.g. patellogastropod limpets and the Littorinidae (Hedegaard et al., 1997; Taylor and Reid, 1990), have, in addition to aragonitic shell layers, evolved outer calcitic shell layers. It was argued that calcitic shell layers are an adaptation to resist dissolution (Taylor and Reid, 1990). The latter hypothesis was questioned on the basis of a comparative dissolution study using aragonitic and calcitic bivalve microstructures (Harper, 2000). Comparing the post-mortem dissolution rates of four (two aragonitic and two calcitic) Antarctic benthic species, McClintock et al. (2009) supported the conclusion of Harper (2000). The latter two studies imply the notion that dissolution of calcium carbonate biominerals is not primarily a question of the polymorph, but depends largely on composition and microstructure of the biomineral. As regards the vulnerability to ocean acidification, shell dissolution is merely one aspect, which focuses

entirely on the product, i.e. the shell. The production of the latter is another aspect, and under ocean acidification some organisms might be able to compensate for shell dissolution by increasing shell production (Rodolfo-Metalpa et al., 2011). This compensatory shell production might favour the more dissolution resistant polymorph in species producing both
55 aragonite and calcite (see also Taylor and Reid, 1990). Specimens of the limpet *Patella caerulea*, collected at a highly acidified volcanic CO₂ vent site at Ischia, displayed higher gross calcification rates than their fellow specimens, collected outside the vent site (normal pH, Rodolfo-Metalpa et al., 2011). It was also shown that *P. caerulea* specimens collected within the vent site are considerably corroded (Hall-Spencer et al., 2008; Rodolfo-Metalpa et al., 2011). Taken together the latter two observations suggest that *P. caerulea* might be able to
60 compensate, to a certain extent (compare Hall-Spencer et al., 2008; Rodolfo-Metalpa et al., 2011), shell dissolution by excess shell production. Since limpets produce aragonitic as well as calcitic shell layers (see above), an interesting question is whether compensatory shell production shows a bias towards a particular polymorph. Here we present the polymorph
65 distribution of complete cross sections of *P. caerulea* shells collected from within and outside the Ischia CO₂ vent site (Hall-Spencer et al., 2008; Rodolfo-Metalpa et al., 2011).

2. MATERIAL AND METHODS

2.1. Study site and sampling

70 The study site is an area located off the east coast of Ischia (40°43.81'N, 13°57.98'E), in shallow waters of 2-6 m and within 1-15 m of the shore line. Emissions from the vents in this area are composed of 90–95% CO₂, 3–6% N₂, 0.6–0.8% O₂, 0.2–0.8% CH₄ and 0.08–0.1% Ar, without toxic sulphur compounds (Hall-Spencer et al., 2008). Since the vent gases do not contain toxic substances and are at ambient seawater temperature, this area can be used as a

75 natural laboratory to understand ecosystem effects of ocean acidification. Gas fluxes were
measured during 2006-2007, and no seasonal, tidal or diurnal variation in gas flow rates was
detected, while pH and saturation states of aragonite and calcite varied with sea state, being
lowest on calm days, and showed large decreases as pCO₂ amounts increased proceeding
80 | towards the vent sites (Hall-Spencer *et al.*, 2008). *Patella caerulea* specimens (for
photographs see Figure S1) were collected from two low pH sites (PL1 and PL2), and from a
control site (C) in December 2009 (Figure 1). Temperature, pH and TA were measured from
September to December 2009, and the other carbonate chemistry parameters were calculated
from them. PL1 and PL2 had a mean pH of 6.46 ± 0.35 (mean \pm S.D.) and 6.51 ± 0.38
respectively, while the control site had a mean pH of 8.03 ± 0.05 (Table 1).

85

2.2. Sample preparation and Raman spectroscopy:

Raman imaging was done using a WITec alpha 300 R (WITec GmbH, Germany)
confocal Raman microscope. Imaging was done using a motorized scan table having a
maximum scan range of up to 2.5 x 2.5 cm and a minimum step size of 100 nm. Scans are
90 performed using a 532 nm diode laser and an ultra-high throughput spectrometer with a
grating, 600/mm, and 500 mm blaze (UHTS 300, WITec, Germany). The used objective was
a 20x Zeiss with a NA of 0.4.

For the imaging every 10 μm a Raman spectra was acquired with a integration time of
0.05 s per spectra. The size of the sample and its irregular shape as well as the extremely high
95 resolution of 10 μm (resulting in huge spectral files) did not allow imaging the whole sample
in one run. Therefore the sample had to be repositioned several times. Therefore the sample
processing had to be done for each scan separately (using the WITec Project software, version
2.10). This resulted in slightly different colour scales for each image, since it was not possible

100 to synchronize the latter during the data processing. However, this does only alter the optical
appearance of the images after they have been stitched together using the software Gimp 2.8
and does not affect the interpretation of the images. For details on the Raman imaging of this
type of samples the interested reader is referred to several other publications performed using
the described setup (e.g. Nehrke and Nouet, 2011; Nehrke et al., 2012; Wall and Nehrke,
2012; Stemmer and Nehrke 2014).

105

2.3. Size measurements and data analysis

Transversally sectioned and resin-embedded shells were imaged using a Nikon
SMZ1500 stereo microscope. Shell length and shell thickness were measured using Nikon
110 NIS Elements 4.0 software. All bar-plots show the mean \pm standard deviation of four shells
(four pH_{low}-shells and four pH_n-shells were analysed). Since shells of *P.caerulea* are not
symmetric we always measured the shorter of the two shell flanks. Size normalised thickness
of a shell's shorter flank (SNTF) was determined by averaging ca. 35 evenly spaced thickness
measurements and dividing the resulting value by the shell's length. Size normalised thickness
115 of a shell's apex (SNTA) was determined by averaging ca. 10 evenly spaced thickness
measurements and dividing the resulting value by the shell's length. The apex of a shell was
arbitrarily defined as a certain distance (ca. 1.5 mm) left and right to the highest point of the
shell (see Figure 2). The latter measure was taken to avoid a one-point measurement of the
highest point of a shell. Such a one-point measurement is prone to being not representative.
120 The fraction of aragonite area (FA) was determined as pixels representing aragonite
(measured by means of Nikon NIS Elements 4.0 software) divided by the sum of pixels
representing aragonite and pixels representing calcite (Figure 3). The size normalised

125 aragonite area (SNAA) equals pixels representing aragonite divided by the shell length. The size normalised calcite area (SNCA) equals pixels representing calcite divided by the shell length.

3. RESULTS

130 All shells selected for analysis were of similar size. The length of the pH_n -shells was 31 ± 2 mm (mean \pm standard deviation of four shells), while the length of the pH_{low} -shells was 36 ± 3 mm (mean \pm standard deviation of four shells). Polymorph distribution imaging revealed marked differences between pH_{low} -shells and pH_n -shells (Figure 4). Size normalised thickness of the flank (SNTF) was 26% lower in pH_{low} -shells (Figure 5), while size normalised thickness of the apex (SNTA) was 26% higher in pH_{low} -shells (Figure 6). The fraction of aragonite area (FA) was by a factor of 2.3 higher in pH_{low} -shells (Figure 7). Size normalised aragonite area (SNAA) was by a factor of 2.2 higher in pH_{low} -shells (Figure 8), and size normalised calcite area (SNCA) was by a factor of 2.4 lower in pH_{low} -shells (Figure 9).

4. DISCUSSION

140 The low pH site at Ischia, from which the analysed pH_{low} -shells were taken, features seawater that is under-saturated with respect to both aragonite and calcite (Table 1). Hence shells of calcareous organisms residing in these under-saturated waters are prone to dissolution. Indeed, shells of *P. caerulea* clearly show signs of dissolution (Hall-Spencer et al., 2008; Rodolfo-Metalpa et al., 2011). Therefore, *P. caerulea* pH_{low} -shells are the product of both shell formation and dissolution, as opposed to N-shells (originating from the normal pH site), which are merely the product of shell formation. Provided they grow normally,

pH_{low}-shells should, because of dissolution, display a reduced size normalized thickness (SNT). This is, for the flank area of the shell, indeed the case (Figure 7). On the contrary, in the apex area, the SNT is higher in pH_{low}-shells (Figure 6). The latter can only stem from enhanced shell production. From the above it can be concluded that net shell production in pH_{low}-shells is region-specific, i.e. enhanced at the apex area, and reduced along the flank area. A comparison of the mineralogical composition of the shells from the two different sites shows that the fraction of aragonite area (FA) for pH_{low}-shells is twice as big as for pH_n-shells (Figure 7). This observation could exclusively be due to a higher SNT of the apex area, which is predominantly aragonitic. If the increased FA is related to normal shell production and dissolution, the size normalised aragonite area (SNAA) should be unaltered or decreased. We observed, contrariwise, an increased SNAA (Figure 8), which is in line with the increased SNT of the apex area, both pointing to enhanced shell production. Along the flank area, however, the SNT is decreased in pH_{low}-shells (Figure 7), and so is the overall size normalised calcite area (SNCA, Figure 9). To conclude, there is ample evidence suggesting that low pH exposed *P. caerulea* specimens counteract dissolution by enhanced shell production. Hence the mineralogical analyses of the shell sections support our conclusion drawn on the basis of the thickness measurements, i.e. that enhancement of shell production is region-specific, and, by entailment, polymorph-specific. The latter conclusion is plausible when considering simultaneous shell growth and dissolution as will be detailed in the following.

Under normal pH conditions *P. caerulea* produces shells characterized by a predominately aragonitic apex area and a flank area which is aragonitic and calcitic in the upper part but solely calcitic in the lower part. This is different for shells formed under low pH conditions. The apex area is still predominantly aragonitic but large parts of the flank area are now aragonitic as well (compare Figure 4). This observation is related to the fact that shell

growth and dissolution take place simultaneously during the complete lifespan of *P. caerulea*. Under normal pH conditions the shell is growing by the addition of calcitic material at the edges of the shell flank in form of a cross foliated structure (MacClintock, 1967). With time this material is dissolved which results in a thinning of the shell. Our observations suggest that *P. caerulea* counteracts this thinning by depositing additional layers on the inside-inner side of the shell. Since the deposition of layers at the inside-inner side of the shell is related to a mechanism producing aragonite the amount of aragonite increases while calcitic parts at the outside are dissolved. New formation of calcitic areas is only possible during elongation of the shell (increase in size) but not to counteract dissolution. The scenario described above results in the relative (as expressed by FA, Figure 7) increase in aragonite in the pH_{low}-shells. Taken together with the absolute (as expressed by SNAA, Figure 8) increase in aragonite and the increased SNT of the apex area (Figure 6) in the pH_{low}-shells, this suggests a high efficacy of the compensatory shell production. Our results demonstrate that the ability of limpets to cope, to a certain extent (compare also Hall-Spencer et al., 2008; Rodolfo-Metalpa et al., 2011), with corrosive waters is not related to the preferential usage of the more dissolution resistant polymorph, but is solely governed by the mechanism of shell formation. This mechanism allows for compensatory shell thickening through the deposition of additional layers on the inside-inner side of the shell. We do not know whether the additional layers are structural layers. One possibility is that the layers we call “additional” are similar to the layers related to shell repair in *Haliotis* (Fleury et al. 2008). These additional layers are aragonitic, but this is genetically determined and does not represent a response to ocean acidification. The shift towards aragonite seen in pH_{low}-shells is simply a by-product of the way limpets use calcium carbonate polymorphs in shell formation. The fact that the additional, aragonitic, layers of the pH_{low}-shells lead to an increased SNT of the apex (Figure 6) also shows that aragonite cannot be regarded as a per se disadvantageous polymorph under corrosive ocean acidification. We ascribed the changes in shell mineralogy and shell thickness of our samples

Formatiert: Schriftart: Nicht Fett

Formatiert: Schriftart: Nicht Fett

to seawater carbonate chemistry changes. Since these are field samples, as opposed to experimental samples, possible secondary influences have to be considered. For *Mytilus* it was shown that maybe salinity, but certainly temperature influences the aragonite/calcite ratio (Dodd 1966, Eisma 1966). The latter is also true for *Patella* (Cohen and Branch 1992). In our case, however, both temperature and salinity at the two sites (Figure 1) were the same at any given time (Table 1, Cigliano et al. 2010, Hall-Spencer et al. 2008, Rodolfo-Metalpa et al. 2011), and we conclude that these two parameters did not influence the aragonite/calcite ratio of our samples. Also both the control site and the low pH site we sampled at Ischia are sheltered so that there is no difference in wave action, which could potentially influence shell architecture. Furthermore, it was suggested that the concentrations of inorganic ions such as Mg and Sr can influence the mineralogy of marine calcifying organisms (Watabe 1974). Since salinity was constant in our case, the concentrations of major ions such as Mg and Sr were likewise, and their influence can be ruled out. On the other hand, shells from the low pH site clearly are corroded (see above), so there is a massive impact of seawater carbonate chemistry on the organism. Taken together with the constancy of other environmental parameters, that leads us to conclude that carbonate chemistry changes are the best explanation for the changes in shell mineralogy and shell thickness of our samples.

5. Conclusion

Polymorph distribution analyses of complete cross sections of *Patella caerulea* shells from a CO₂ vent site at Ischia revealed that this species counteracts shell dissolution in corrosive waters by enhanced production of aragonitic shell layers. The question whether these layers represent structural layers will be the subject matter of an upcoming microstructural investigation.

Formatiert: Schriftart: Nicht Fett, Kursiv

Formatiert: Schriftart: Nicht Fett

Formatiert: Schriftart: Nicht Fett, Kursiv

Formatiert: Schriftart: Nicht Fett

Formatiert: Schriftart: 14 Pt., Fett

Formatiert: Zentriert

Formatiert: Schriftart: Nicht Fett

Formatiert: Einzug: Erste Zeile: 1,27 cm

Acknowledgements

No acknowledgements at this stage

225 **References**

Bednarsek N., Tarling G. A., Bakker D. C. E., Fielding S., Jones E. M., Venables H. J., Ward P., Kuzirian A., Leze B., Feely R. A., and Murphy E. J. (2012) Extensive dissolution of live pteropods in the Southern Ocean. *Nature Geoscience* **5**(12), 881-885.

230 Cigliano, M; Gambi, Maria Cristina; Rodolfo-Metalpa, Riccardo; Patti, F P; Hall-Spencer, Jason M (2010): Effects of ocean acidification on invertebrate settlement at volcanic CO2 vents. *Marine Biology*, 157(11), 2489-2502

Cohen, A.L., Branch, G.M. (1992) Environmentally controlled variation in the structure and mineralogy of *Patella granularis* shells from the coast of southern Africa: implications for palaeotemperature assessments. *Palaeogeography, Palaeoclimatology, Palaeoecology*, Volume 91, Pages 49-57

235 Dodd, J.R. (1966) The Influence of Salinity on Mollusk Shell Mineralogy: A Discussion. *The Journal of Geology*, Vol. 74, pp. 85-89

Eisma, D. (1966) The Influence of Salinity on Mollusk Shell Mineralogy: A Discussion. *The Journal of Geology*, Vol. 74, pp. 89-94

240 Field C. B., Barros V., Stocker T. F., Dahe Q., Mach K. J., Plattner G., Mastrandrea M. D., Tignor M., and Ebi K. L. (2011) IPCC Workshop on Impacts of Ocean Acidification on Marine Biology and Ecosystems, 164pp.

Fleury, C., Marin, F, Marie, B, Luquet, G, Thomas, J., Josse, C., Serpentine, A., Lebel, J.M. (2008) Shell repair process in the green ormer *Haliotis tuberculata*: A histological and microstructural study. *Tissue and Cell* **40**, 207-218

Gattuso J.-P. and Hansson L. (2011) *Ocean Acidification*. Oxford University Press.

- Formatiert:** Schriftart: Nicht Fett
- Formatiert:** Schriftart: Nicht Fett
- Formatiert:** Schriftart: Nicht Fett, Kursiv
- Formatiert:** Schriftart: Nicht Fett
- Formatiert:** Schriftart: Nicht Fett
- Formatiert:** Schriftart: (Standard) Times New Roman, 12 Pt., Englisch (USA)
- Formatiert:** Links, Abstand Nach: 0 Pt., Trennen, Tabstopps: 1,62 cm, Links + 3,23 cm, Links + 4,85 cm, Links + 6,46 cm, Links + 8,08 cm, Links + 9,69 cm, Links + 11,31 cm, Links + 12,92 cm, Links + 14,54 cm, Links + 16,16 cm, Links + 17,77 cm, Links + 19,39 cm, Links + 21 cm, Links + 22,62 cm, Links + 24,23 cm, Links + 25,85 cm, Links
- Formatiert:** Schriftart: (Standard) Times New Roman, 12 Pt., Englisch (USA)
- Formatiert:** Schriftart: (Standard) Times New Roman, 12 Pt., Englisch (USA)
- Formatiert:** Schriftart: (Standard) Times New Roman, 12 Pt., Englisch (USA)
- Formatiert:** Schriftart: (Standard) Times New Roman, 12 Pt., Englisch (USA)
- Formatiert:** Schriftart: (Standard) Times New Roman, 12 Pt., Englisch (USA)
- Formatiert:** Schriftart: (Standard) Times New Roman, 12 Pt., Englisch (USA)
- Formatiert:** Schriftart: (Standard) Times New Roman, 12 Pt., Englisch (USA)
- Formatiert:** Schriftart: (Standard) Times New Roman, 12 Pt., Englisch (USA)
- Formatiert:** Schriftart: (Standard) Times New Roman, 12 Pt., Englisch (USA)
- Formatiert:** Schriftart: (Standard) Times New Roman, 12 Pt., Englisch (USA)
- Formatiert:** Schriftart: 12 Pt., Englisch (USA)

- Hall-Spencer J. M., Rodolfo-Metalpa R., Martin S., Ransome E., Fine M., Turner S. M., Rowley S. J., Tedesco D., and Buia M.-C. (2008) Volcanic carbon dioxide vents show ecosystem effects of ocean acidification. *Nature* **454**(7200), 96-99.
- 250 Harper E. M. (2000) Are calcitic layers an effective adaptation against shell dissolution in the Bivalvia? *Journal of Zoology* **251**, 179-186.
- Hedegaard C., Lindberg D. R., and Bandel K. (1997) Shell microstructure of a Triassic patellogastropod limpet. *Lethaia* **30**, 331-335.
- 255 MacClintock, C. (1967) Shell Structure of Patelloid and Bellerophonoid Gastropods (Mollusca). Peabody Museum of Natural History Yale University Bulletin 22, New Haven, Connecticut
- McClintock J. B., Angus R. A., McDonald M. R., Amsler C. D., Catledge S. A., and Vohra Y. K. (2009) Rapid dissolution of shells of weakly calcified Antarctic benthic macroorganisms indicates high vulnerability to ocean acidification. *Antarctic Science* **21**(05), 449-456.
- 260 McNeil B. I. and Matear R. J. (2008) Southern Ocean acidification: A tipping point at 450-ppm atmospheric CO₂. *Proceedings of the National Academy of Sciences* **105**(48), 18860-18864.
- Nehrke, G. and Nouet J. (2011) Confocal Raman microscope mapping as a tool to describe different mineral and organic phases at high spatial resolution within marine biogenic carbonates: case study on *Nerita undata* (Gastropoda, Neritopsina). *Biogeosciences* **8** (12): p. 3761-3769.
- 265 Nehrke, G., Poigner H., Wilhelms-Dick D., Brey T., and Abele D. (2012) *Coexistence of three calcium carbonate polymorphs in the shell of the Antarctic clam *Laternula elliptica**. *Geochem. Geophys. Geosyst.* **13**: p. Q05014.
- Orr J. C., Fabry V. J., Aumont O., Bopp L., Doney S. C., Feely R. A., Gnanadesikan A., Gruber N., Ishida A., Joos F., Key R. M., Lindsay K., Maier-Reimer E., Matear R., Monfray P., Mouchet A., 270 Najjar R. G., Plattner G.-K., Rodgers K. B., Sabine C. L., Sarmiento J. L., Schlitzer R., Slater R. D., Totterdell I. J., Weirig M.-F., Yamanaka Y., and Yool A. (2005) Anthropogenic ocean acidification over the twenty-first century and its impact on calcifying organisms. *Nature* **437**(7059), 681-686.

Rodolfo-Metalpa R., Houlbreque F., Tambutte E., Boisson F., Baggini C., Patti F. P., Jeffree R., Fine M., Foggo A., Gattuso J.-P., and Hall-Spencer J. M. (2011) Coral and mollusc resistance to ocean acidification adversely affected by warming. *Nature Climate Change* **1**(6), 308-312.

Royal Society (2005) Ocean acidification due to increasing atmospheric carbon dioxide, pp. 60. Policy Document 12/05, The Royal Society, London.

Stemmer, K. and Nehrke G. (2014) *THE DISTRIBUTION OF POLYENES IN THE SHELL OF ARCTICA ISLANDICA FROM NORTH ATLANTIC LOCALITIES: A CONFOCAL RAMAN MICROSCOPY STUDY*. *Journal of Molluscan Studies* **80**, 365-370. doi:10.1093/molus/eyu033

Taylor J. D. and Reid D. G. (1990) Shell microstructure and mineralogy of the Littorinidae: ecological and evolutionary significance. *Hydrobiologia* **193**, 199-215.

Wall, M. and Nehrke G. (2012) *Reconstructing skeletal fiber arrangement and growth mode in the coral Porites lutea (Cnidaria, Scleractinia): a confocal Raman microscopy study*. *Biogeosciences* **9**(11): p. 4885-4895.

Watabe, N. (1974) Crystal growth of calcium carbonate in biological systems, Journal of Crystal Growth, Volumes 24–25, Pages 116-122

Formatiert: Schriftart: Nicht Fett

TABLES

290 Table 1. Mean value (\pm S.D.) of temperature (T), pH (total scale), pCO₂, concentration of HCO₃⁻ and CO₃²⁻ ions, CO₂ concentration in sea water, dissolved inorganic carbon (DIC), saturation state (Ω) of aragonite and calcite for the study sites.

Site	T (°C)	pH _T	pCO ₂ (μ atm)	HCO ₃ ⁻ (μ mol/kg)	CO ₃ ²⁻ (μ mol/kg)	CO ₂ (μ mol/kg)	DIC (μ mol/kg)	Ω_{Ca}	Ω_{Ar}
C	19.7 (\pm 2.0)	8.03 (\pm 0.05)	474 (\pm 74)	2043 (\pm 46)	220 (\pm 19)	15 (\pm 2)	2279 (\pm 29)	5.15 (\pm 0.45)	3.36 (\pm 0.30)
PL1	20.1 (\pm 2.2)	6.46 (\pm 0.35)	22047 (\pm 13264)	2542 (\pm 50)	14 (\pm 21)	758 (\pm 510)	3315 (\pm 526)	0.33 (\pm 0.48)	0.22 (\pm 0.32)
PL2	20.1 (\pm 2.2)	6.51 (\pm 0.38)	19504 (\pm 12338)	2509 (\pm 96)	17 (\pm 18)	618 (\pm 392)	3143 (\pm 426)	0.39 (\pm 0.43)	0.26 (\pm 0.28)

295

FIGURE CAPTIONS

Figure 1. Map of the study area, showing the low pH sites (PL1 and PL2) and the control site (C).

Figure 2: Sketch of a shell indicating length, apex, and shortest flank.

300 Figure 3: Example of a Raman image across the cross section of the Shell. Blue represents aragonite and yellow calcite, as identified by the corresponding Raman spectra shown.

Figure 4: Polymorph distribution of transversally sectioned shells. Blue = aragonite, yellow = calcite. Normal = pH_n -shells, Low = pH_{low} -shells.

Figure 5: Size normalised thickness of the flank (SNTF). Normal = pH_n -shells, Low = pH_{low} -
305 shells.

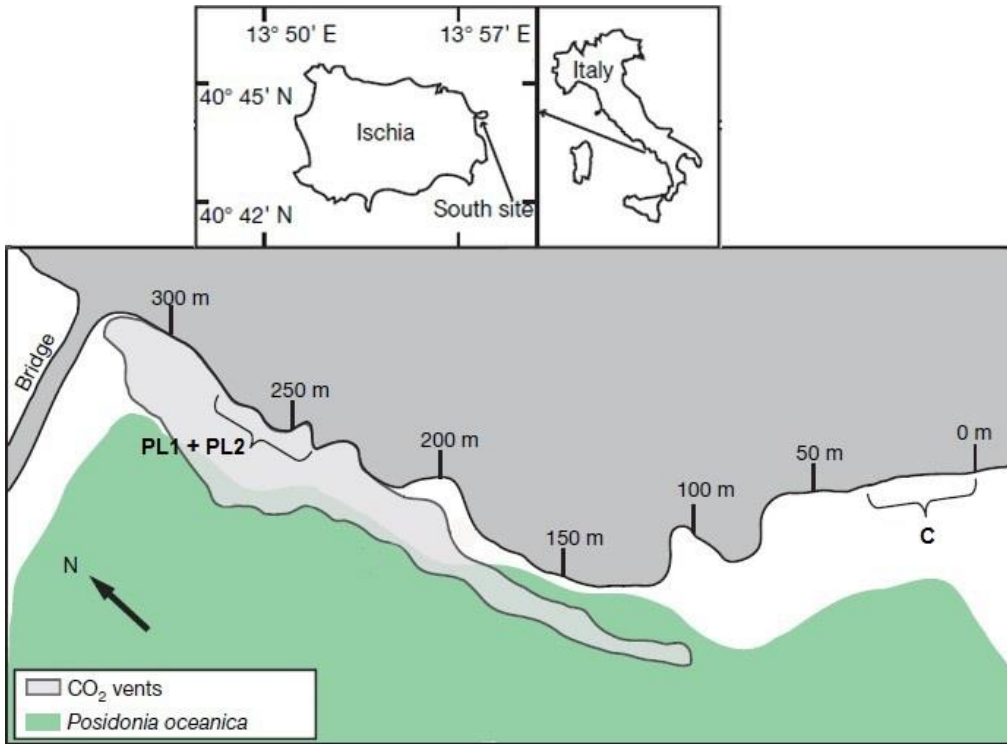
Figure 6: Size normalised thickness of the apex (SNTA). Normal = pH_n -shells, Low = pH_{low} -shells.

Figure 7: Fraction of aragonite area (FA). Normal = pH_n -shells, Low = pH_{low} -shells.

Figure 8: Size normalised aragonite area (SNAA). Normal = pH_n -shells, Low = pH_{low} -shells.

310 Figure 9: Size normalised calcite area (SNCA). Normal = pH_n -shells, Low = pH_{low} -shells.

Figure 1



315 Figure 2:

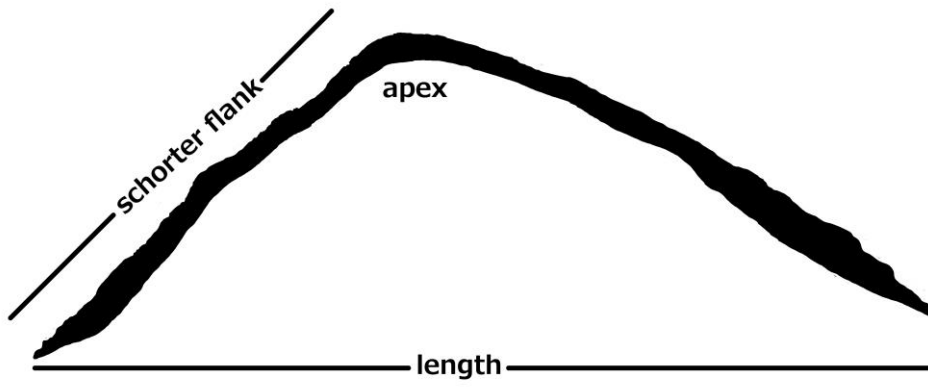
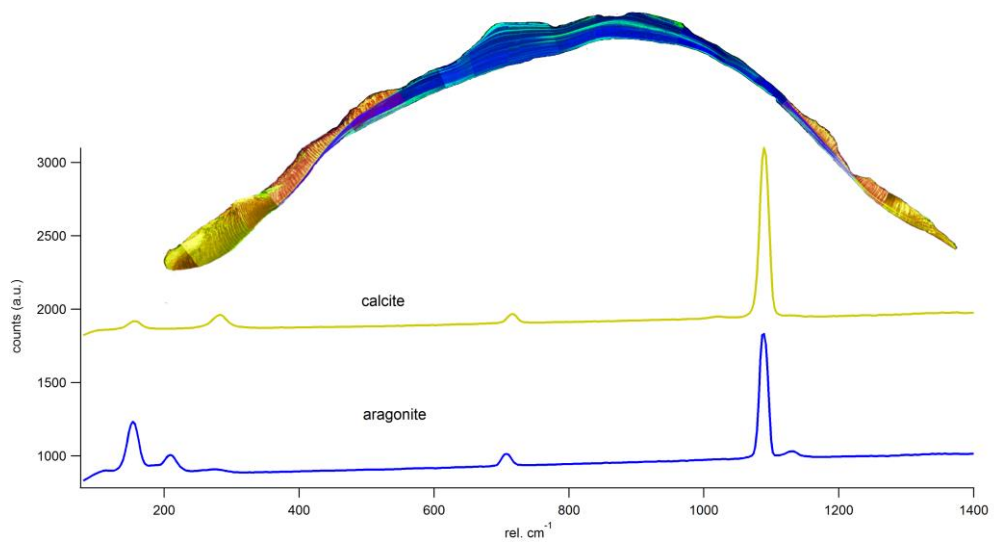
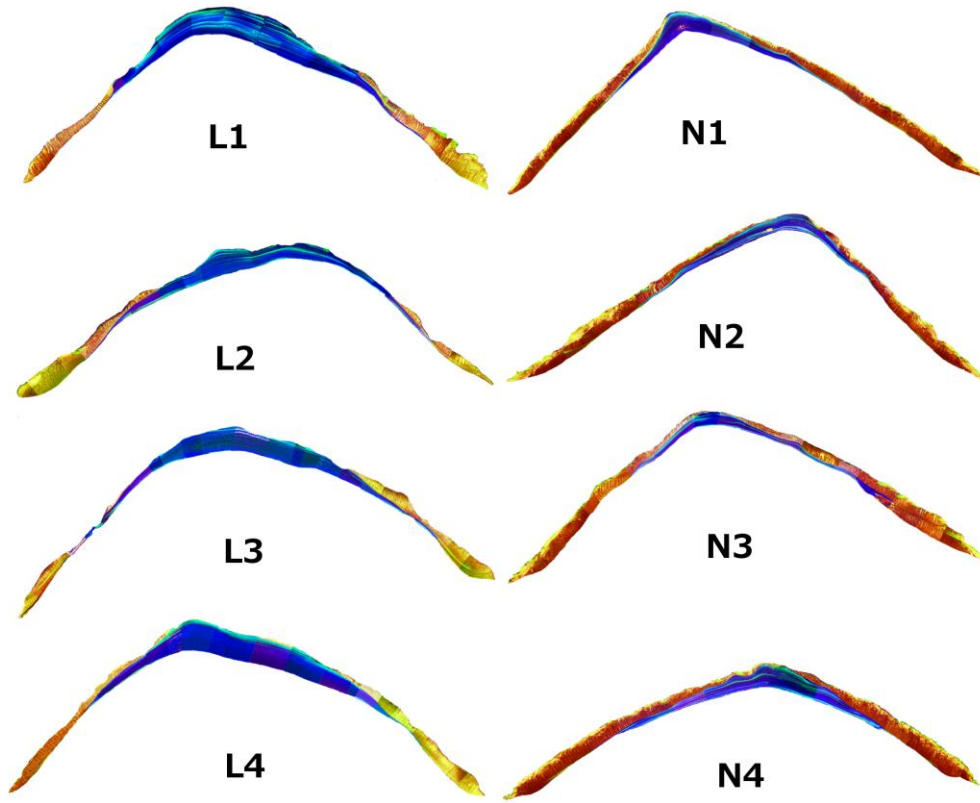


Figure 3:



320

Figure 4:



325 Figure 5:

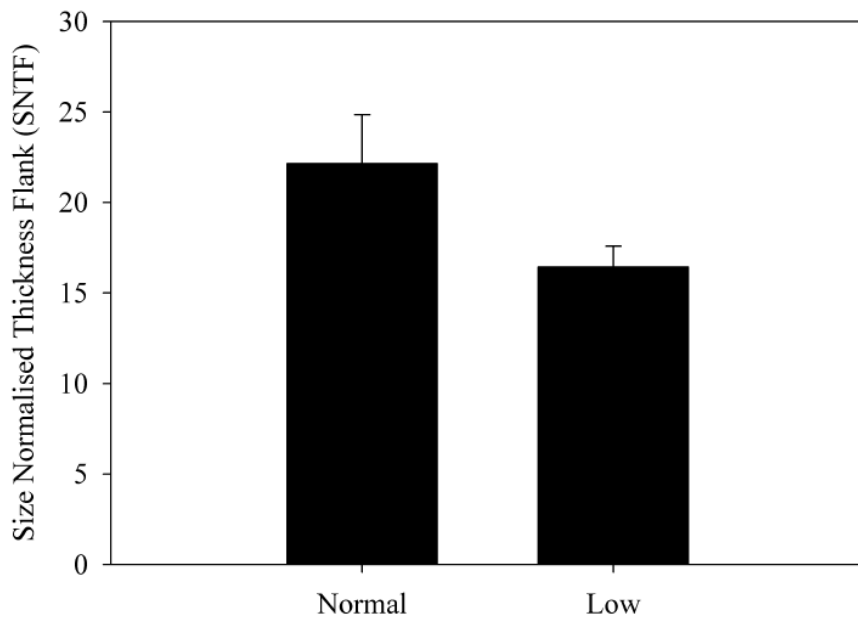


Figure 6:

330

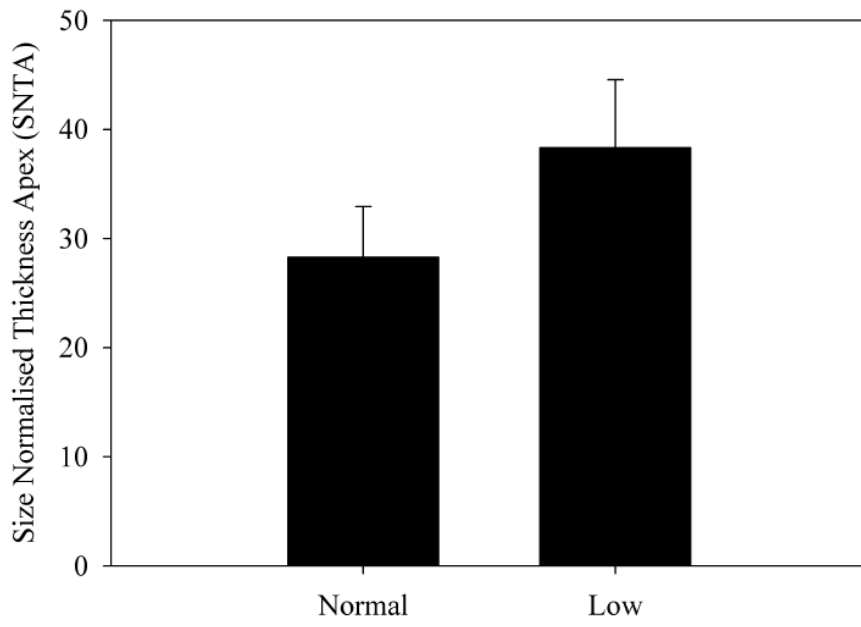
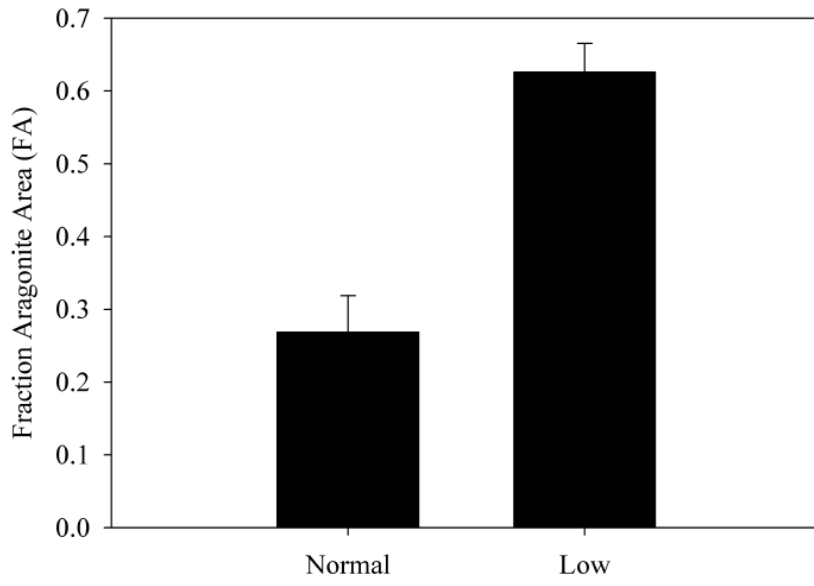
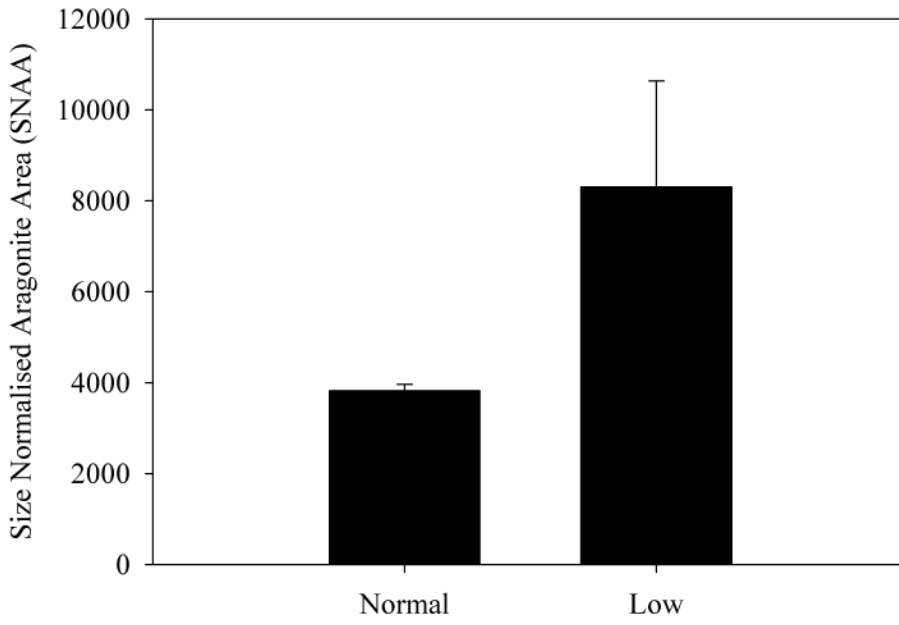


Figure 7:



335

Figure 8:



340

Figure 9:

